STUDY OF DIELECTRIC BARRIER DISCHARGE IN AIR AND ESTIMATION OF ELECTRON DENSITY AND ENERGY DEPOSITION

Bhesh Bahadur Thapa[1] and Raju Bhai Tyata[1]

[1]*Department of Science and Humanities, Khwopa College of Engineering, Libali-8, Bhaktapur, Nepal*

Abstract

This paper reports the electrical behaviors of atmospheric pressure plasma reactor with Dielectric Barrier Discharge (DBD) in air medium. The DBD discharge was generated in air at atmospheric pressure using Disc Electrode Geometry (DEG) reactor powered by ac voltage (0-7kV) at a frequency of 24kHz. The glass plates of thickness 1.0mm and 3.0mm were used as dielectric. The current-voltage characteristics were studied for two air gap of 2.0mm and 3.0mm by varying the applied voltages. The numbers of filamentary micro discharges were found as increased in each half cycle with increase in power. The observations of Lissajous figure of applied voltage versus electric current was used for measuring energy deposited by discharge and also compared with calculated value. Lissajous figures clearly show that the energy deposited by discharge was dependent on applied voltage. The electron density of discharge was measured by power balance method. Electron density was found in the order of 10^{17}per cubic meter.

Keywords: DBD, Filamentary Discharge, Atmospheric Pressure, Energy Deposited, Lissajous Figure.

1. Introduction

In DBD electrical discharge is generated between two electrodes (at least one is covered by an electrical insulator). Common materials for dielectric barriers are glass, quartz, ceramics, or enamels. Also, plastic films, silicon rubber, teflon plates and other materials can be used. Its first experimental investigation was reported by Werner Von Siemens in 1857 for ozone generation (Konelschatz et al., 1997). The atmospheric pressure DBD typically operates in the filamentary mode (Brandenburg et al., 2009; Dramane et al., 2008; Sun et al., 2012), but under specific operating conditions, it is also possible to operate in a diffused mode, where spatial homogeneity in the direction parallel to the electrodes is obtained. This enables the discharge to be used for homogeneous surface treatments at atmospheric pressure (Tyata et al., 2014; Xiaoping et al., 2012). The DBD has been an interesting subject for many researchers because of its simplicity in operation and great potential in industrial applications.

*Corresponding author: Bhesh Bahadur Thapa
Khwopa College of Engineering, Libali-8, Bhaktapur, Nepal
Email: bhesh.thapa09@gmail.com
(Received: Aug 07, 2019 Accepted: November 06, 2019)

DBDs have been widely used in ozone generation (Pekarek, 2012; Tyata et al., 2016), surface treatment of materials (Liu et al., 2018), thin film deposition (Dong-Ling et al., 2018), air purification (Lopez-Fernandez et al., 2017), chemical reactions as chemical reactor (Tay et al., 2014), water treatment (Gyawali et al., 2018), biological applications. DBDs are also used in the design of high power CO_2 lasers, ultraviolet (UV) and vacuum ultraviolet (VUV) excimer lamps and plasma display panels (Yahila, 2016).

It consists of large number of micro-discharges (filaments) with short duration some tens of nanoseconds and sub millimeter size (Brandenburg et al., 2009; Xiaoping et al., 2012).

2. Electrical Breakdown Process in Gases

The electrical breakdown technique is a complicated process of formation of conductive gas channel which occurs when electric field exceeds some critical value (breakdown voltage). Paschen discovered the relationship among the breakdown voltage, gas pressure and gap distance between the parallel plates (Kennedy and Fridman, 2004). This

law shows the breakdown voltage as a function of pressure and inter-electrode distance as represented by equation 1.

$$V_B = \frac{B(pd)}{C + \log(pd)} \quad (1)$$

Where $C = \log\left(\frac{A}{\log(1+1/\gamma)}\right)$ and $V_B = Ed$, the total voltage applied between two electrodes. *A* and *B* are constants depending on the gas used. The secondary emission coefficient γ depends on the cathode material, the state of its surface, type of gas and reduced electric field.

The mechanism of formation of filament correlates with the streamer breakdown theory for spark discharges as shown in Fig.1 (Tyata, 2013).First, a primary electron accelerated by the applied electric field E produces secondary electrons by ionization of gas particles. This leads to an electron avalanche from cathode to anode and produces its own electric field of space charge E_{SC} as shown in Fig. 1(a). The scale of electron avalanche exponentially increases and electron density near the anode becomes much larger than other regions (Liu et al., 2018). When a space charge field E_{SC} is equal or greater than the external field E it causes the transition of avalanche to self-propagating ionized streamer at the anode as shown in Fig. 1(b). The streamer is reflected at the anode due to high space charge at the streamers head and propagates towards the cathode. By bridging the gap, the streamer forms a conductive ion channel with maximum current flow for some nanoseconds as shown in Fig. 1(d).

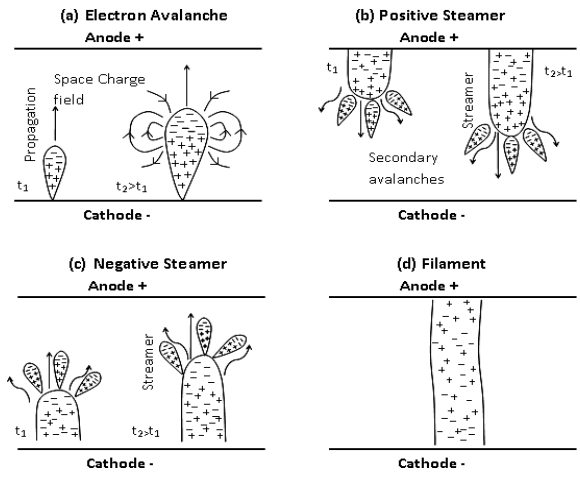

Fig. 1 Streamer mechanism of micro-discharges in DBD

At this point, the micro-discharge appears visible due to emission of photon. Charges are accumulated at the dielectric surface observed as lateral filament spreading and reduce the electric field to such a degree that it collapses within nanoseconds. As the current is terminated, the ionization process stops and the micro-discharge is extinguished (Raizer, 1991).Besides, the surface charges and ionic charges are present in this region (cathode) after termination. These sustained charges allow the formation of a new micro-discharge at the same location when the polarity of the applied voltage is reversed.

The filaments can be observed with our naked eyes. These filaments do not overlap but repel each other. The number of micro-discharges depends on the power density. The higher power causes the distribution of more micro-discharges over the dielectric surface that prevents sparking or arcing. Plasma filaments are also formed without any dielectric. In this case, no surface charges are accumulated at the surface of electrode, and widening of the filamentary channel is prohibited.

After the reversal of polarity of applied voltage, due to accumulation of charges on the surface, non-homogeneous electric field leads the formation of discharge at the same location as those occurred during the previous half cycle. More discharge channels can be generated by increasing applied voltage (Pavon, 2008; Kudu et al., 2008).Fig.2 shows the schematic diagram that shows six time intervals for pause mode and active mode of discharge mechanism between electrodes during a complete cycle of applied ac voltage (Yahia, 2016).

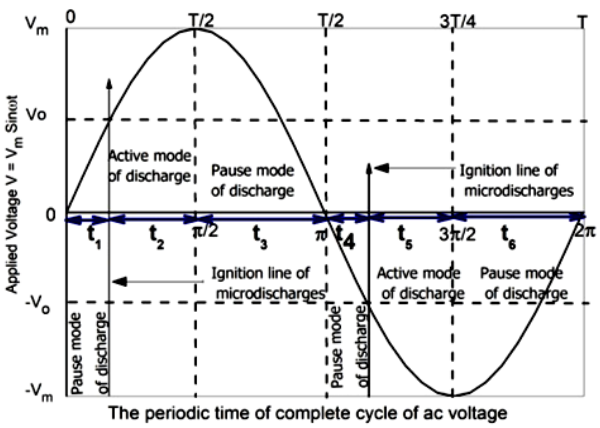

Fig. 2 Active and pause mode of DBD discharge during a complete cycle of applied ac voltage.

Under certain conditions such as gas mixture, frequency of applied voltage, properties of external electric circuit and power supply uniform discharges (called diffused barrier discharges) can be generated (Sun et al., 2012).However the electrical properties of a filamentary discharge are more complicated than homogenous discharge mode. In filamentary discharge, micro-discharges are distributed randomly across the electric field whereas in homogenous Townsend discharge a single discharge covers the entire discharge region (Tyata et al., 2014; Wang et al., 2012).

Manley designed an experimental technique for the first time to measure electric power that is consumed in forming the micro-discharges by plotting electric charge versus ac peak voltage which is applied to DBD reactors (Yahila, 2016). This technique is called voltage charge Lissajous figure. It is a precise method for measuring the electrical characteristics for DBDs. The advantage of this technique is that it does not depend on specifications of oscilloscope used in conducting experiments. The closed area of Lissajous figure always represents the electric energy consumed in forming the micro-discharges during a complete cycle of the ac voltage.

Here, an electrical model is used for calculating electrical parameters of DBDs in air at atmospheric conditions. The wave forms of current versus applied voltage were used to obtain the information about ignition and decay of micro-discharges. Also, the current-voltage Lissajous figures were used to calculate the discharge power in one cycle of applied ac voltage.

3. Experimental Setup

The schematic diagram of experimental arrangement used to study the DBD is shown in Fig.3. The discharge is generated between two symmetric circular disc copper electrodes of diameter 4.8cm and thickness 4mm held parallel each other. We get filamentary DBD in air when the ac voltage is applied. If the electrode surface is rough and with sharp edges, to avoid the action of point due to rough and sharp edges on the electrode surface, smooth disc electrode system has been designed. The lower plate is fixed and the upper plate is movable with pitch 0.5mm. Glass plate of thickness 1mm and 3mm were used as a dielectric.

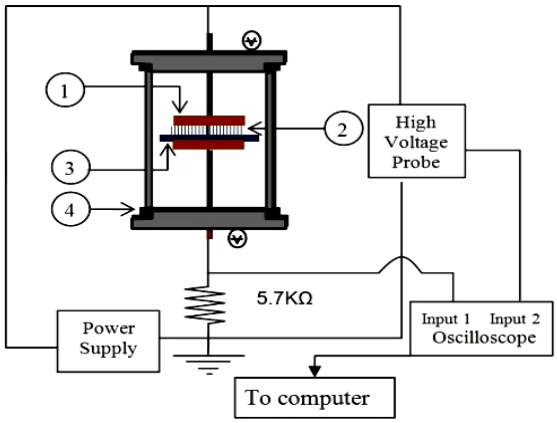

Fig. 3 Schematic diagram of experimental setup (1) Disc Electrode, (2) Discharge, (3) Dielectrics and (4) Chamber

A high voltage ac power supply was used, and the applied voltage was manually increased in the range of 0-7kV peak to peak at a constant frequency 24kHz. The air gap between the electrodes was varied from 2-4mm at atmospheric air pressure. The applied voltage was varied at constant frequency. Electrical characterization was made with the help of a high voltage probe using OWON digital oscilloscope.

4. Result and Discussion

4.1.Discharge Characteristics of DBD

Fig.4a and Fig.4b show photographs of sample discharges in air at atmospheric pressure at constant gap of air 3mm for a 1mm glass as dielectric when applied ac voltage is manually increased. This shows the intensity of barrier discharge increases as the applied voltage is increased.

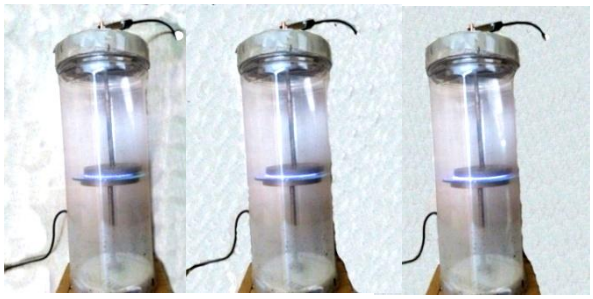

Fig. 4(a)

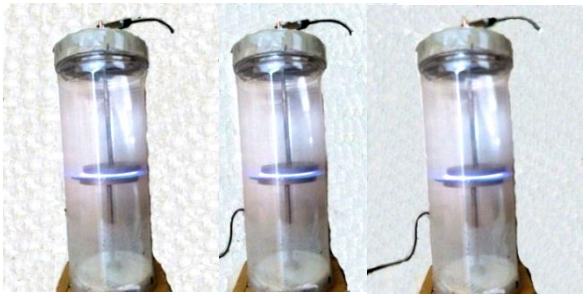

Fig. 4(b)

Fig. 4(a) and 4(b) Photographs of sample discharge (air gap 3mm, glass dielectric of thickness 1mm and atmospheric pressure) at manually increasing applied voltage.

The voltage and current waveforms of the air discharge at manually varying applied voltage were recorded on the oscilloscope as function of time. The square current waveforms were found. This indicates the discharge is in filamentary mode. The current waveform consists of large number of current discharge pulses per half cycle.

From Figs. 5 and 6, it can be observed that by using the glass dielectric, a streamer discharge was formed which is characterized by discrete current spikes. These spikes are related to the formation of micro-discharges in the air space at constant frequency of applied voltage of 24kHz. The current variation is very rapid, and the discharge duration is shorter than 100ns (Xiaoping et al., 2012). In air the discharge current in the positive half cycle is nearly the same as that in the negative half cycle.

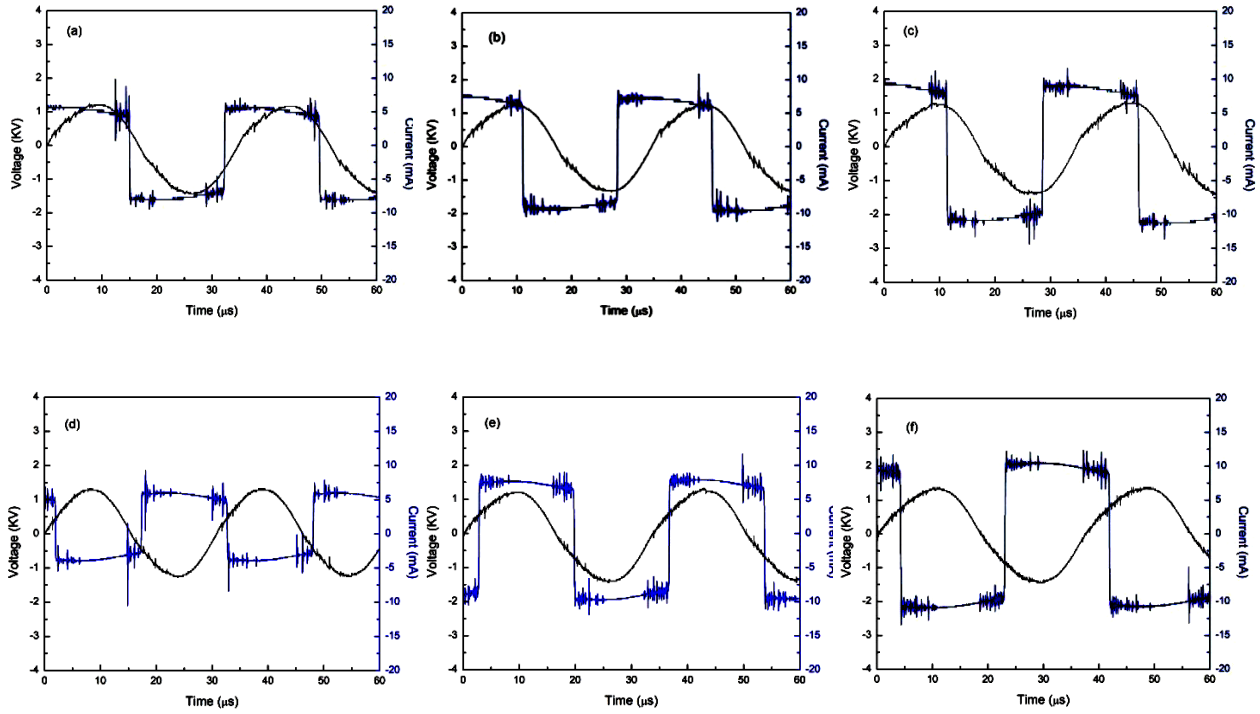

Fig.5 Voltage and current waveforms in air with 2mm gap (a-c) and 3mm gap (d-f) by varying applied voltage 0-7kV at 24kHz using 1mm thick glass as dielectric

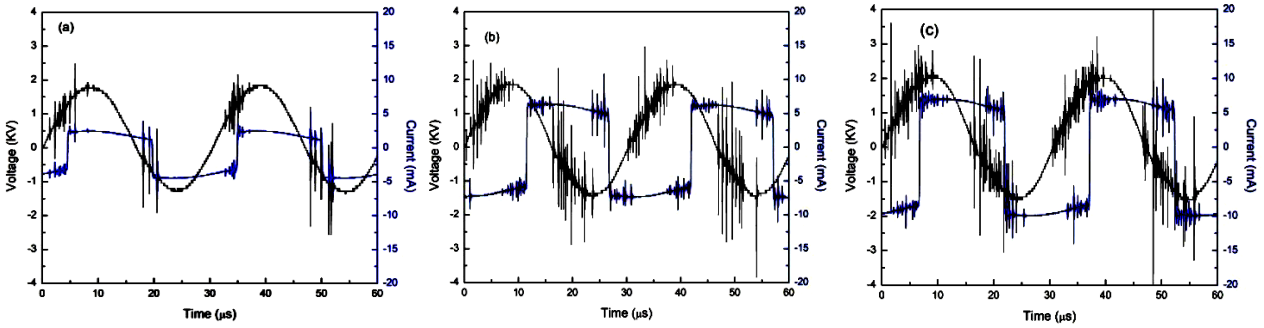

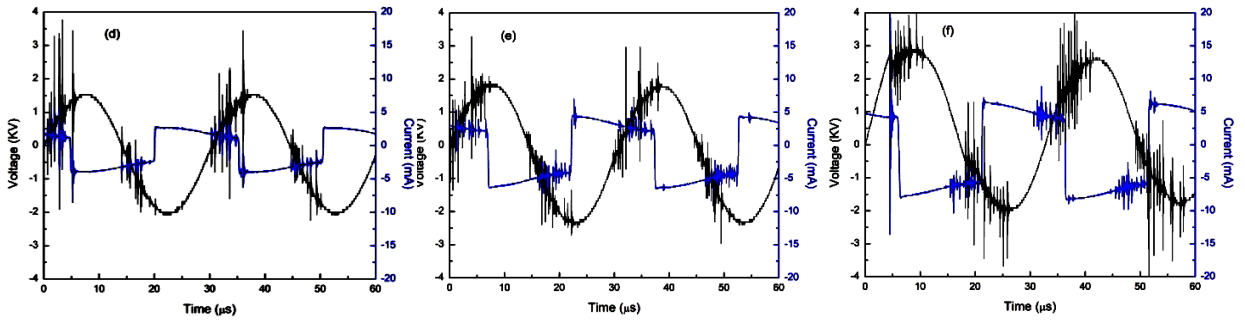

Fig.6 Voltage and current waveforms in air with 2mm gap (a-c) and 3mm gap (d-f) by varying applied voltage 0-7kV at 24kHz using 1mm thick glass as dielectric

Fig. 5(a-c) correspond to discharges with 2mm gap between electrodes whereas Fig. 5(d-f) correspond to gap 3mm using 1mm thick glass as dielectric at different applied voltage. Similarly, Fig.6(a-c) correspond to discharges with 2mm gap between electrodes whereas Fig. 6(d-f) correspond to gap 3mm using 3mm thick glass as dielectric at different applied voltage. The micro-discharges are generated when applied voltage exceeds the breakdown voltage of air. It was found as the applied voltage above breakdown voltage is increased the number of current spikes, and amplitude of current pulses are also increased. The micro-discharges will be extinguished when the charge build up on the dielectric reduces the local electric field. It seems that the breakdown voltage decreases, and the dielectric voltage increases. At any moment, during discharge pulse the voltage equality $V_{app} = V_g + V_D$ is realized, where V_{app} = applied voltage, V_g = gap voltage and V_D = discharge voltage. The role of dielectric is to suppress the discharge at the end of each half cycle.

4.2. Discharge Power

The plot between the charge transferred during the discharge and applied voltage is used to calculate energy consumed per cycle. This plot is called Lissajous figure. Here, we considered applied voltage and discharge current to find discharge power.

It can be seen that the discharge power increases as the applied voltage increases. This effect can be associated with increased number of micro-discharges per unit time. From Figs.7 and 8, the area under the curve gradually increases as applied alternating voltage is increased.

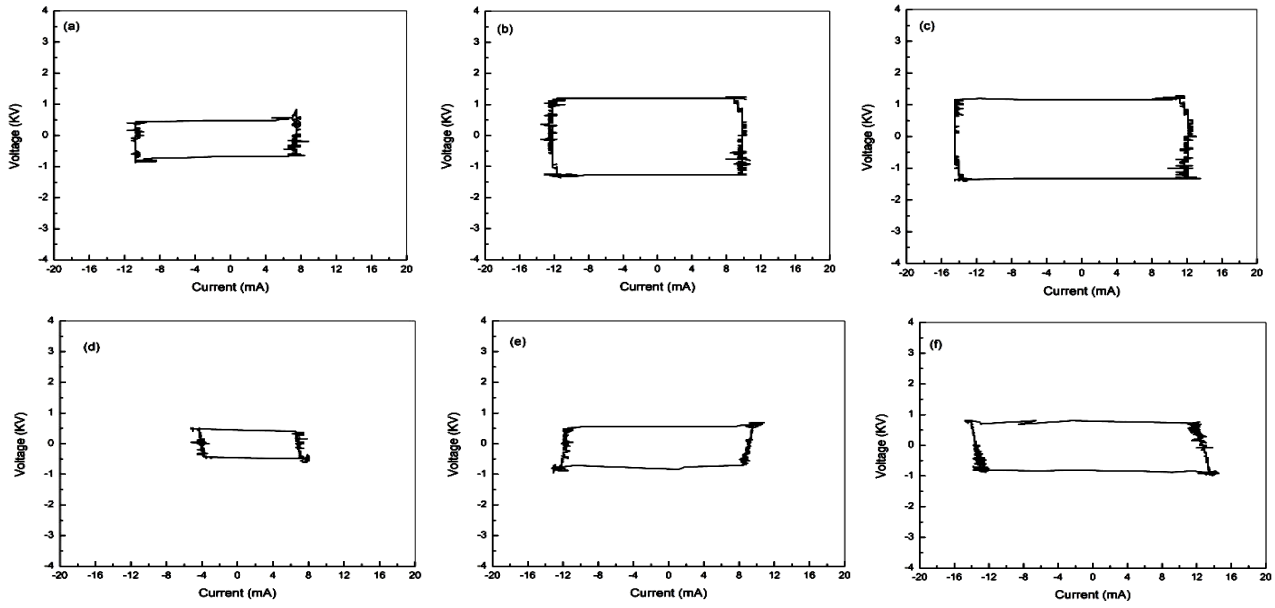

Fig.7 Voltage - current curve in air medium with 2mm gap (a-c) and 3mm gap (d-f) by varying applied voltage 0-7kV at 24kHz using 1mm thick glass as dielectric

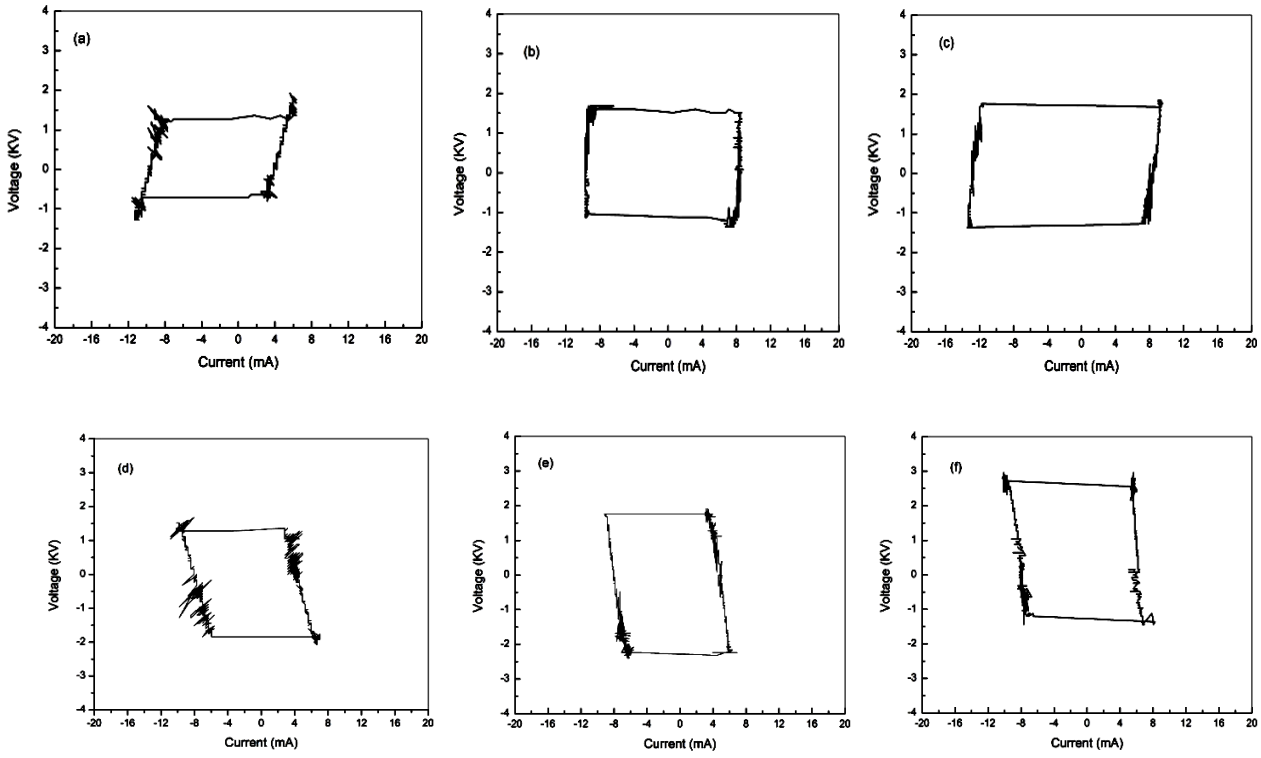

Fig.8 Voltage - current curve in air medium with 2mm gap (a-c) and 3mm gap (d-f) by varying applied voltage 0-7kV at 24kHz using 3mm thick glass as dielectric

4.3. Estimation of Power Consumed

The discharge power *P* can be calculated from the discharge voltage *V* and current I using equation 2.

$$P(t) = V(t) \times I(t) \quad (2)$$

As both the quantities are function of time, the average power can be calculated from integration of the instantaneous power divided by time period given by equation 3 (Xiaoping et al., 2012)

$$P = \frac{1}{T}\int_0^T IVdt = fC\int_s Vdv \quad (3)$$

So, the discharge power can be determined from the area of discharge voltage versus current for ac excitation over a period. From current-voltage plots of Fig. 7 and Fig. 8 observation data of discharge voltage V_{pp}, discharge current I_{pp}, power consumed in one cycle from calculation and power consumed in one cycle using area enclosed by Lissajous figures were tabulated in Table 1 and Table 2 for 2mm glass and 3mm glass as dielectric respectively. From power consumed per cycle of ac, applied voltage in DBD was found increase with increasing applied voltage. Also, it was found that the area of the Lissajous curve decreases with increase in gap at same applied voltage.

Fig. 9 and Fig. 10 show the variation of power consumed with applied voltage.

Table 1 The theoretical calculated and measured values from Fig. 7(a-f) were tabulated in below.

S.N.	Discharge voltage V_{pp} (kV)		Discharge Current I_{pp} (mA)	Power Calculated by the formula $P = V_{pp} \times I_{pp}$ (watt)	Power by enclosed area of Lissajous figure (watt)
1	2mm gap	2.60	13.33	34.66	22.53
2		2.68	16.83	45.10	50.69
3		2.72	19.64	53.42	65.54
4	3mm gap	2.56	9.82	25.14	10.76
5		2.68	16.80	45.02	26.62
6		2.80	21.18	59.30	42.00

Table 2 The theoretical calculated and measured values from Fig. 8(a-f) were tabulated in below.

S.N.	Discharge voltage V_{pp} (kV)		Discharge Current I_{pp} (mA)	Power by formula $P = V_{pp} \times I_{pp}$ (watt)	Power by enclosed area of Lissajous figure (watt)
1	2mm gap	3.2	6.87	21.98	27.64
2		3.36	13.47	45.26	45.06
3		3.6	16.84	60.62	62.98
4	3mm gap	3.52	6.31	22.21	41.48
5		4.24	9.68	41.04	50.68
6		4.64	13.62	63.2	53.24

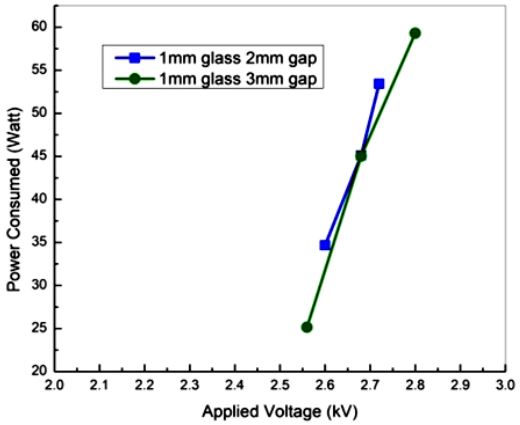

Fig.9 Power consumed by DBD

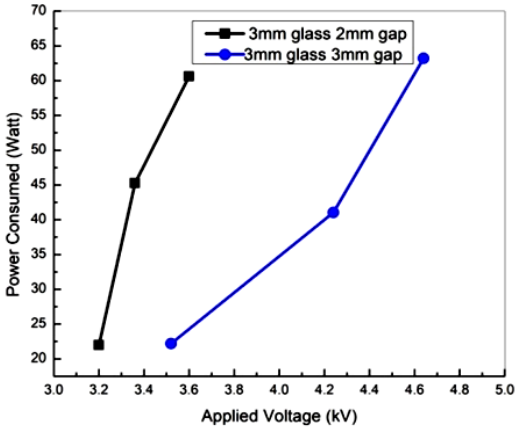

Fig.10 Power consumed by DBD

4.4 Estimation of Electron Density

The electron density can be estimated by power balance method as given by equation 4.

$$n_e = \frac{P_{av}}{2AV_bE_{lost}} \qquad (4)$$

where n_e is electron density, P_{av} is average power, A is area of electrode, V_b is Bohm velocity equal to ion acoustic velocity ~2×10^5 cms^{-1} and total energy lost by the plasma per electron-ion pair energy Elost is 50eV(Balcon et al., 2007). In our DBD reactor, area of electrode A is 18.01 cm2.

From the current-voltage wave forms of Fig. 6 and Fig. 7, detailed observation data of rms voltage and current for positive and two neagative half cycles were tabulated in Table 3 and Table 4 for 1mm thick glass and 3mm thick glass respectively as electrodes for 2mm gap and 3mm gap.

We determined the average electron density by power balance method. We found average electron density in the order of $\approx 10^{17}/m^3$ for 1mm gap and 3mm gap, using glass as a dielectric. This value is quite similar with the results of other researchers (Rajasekaran et al., 2010). Electron density of discharge in air at atmospheric pressure was found increased as the voltage increase. Also the electron density was found low as the gap increased. This is because of weak ionization of air.

Further, correlation coefficients between rms value of applied voltage and electron density for 1mm glass in 2mm gap and 3mm gap were to be found 0.9966, and 0.9923 respectively. Similarly, in case of 3mm glass it was found 0.9789 and 0.9766, for 2mm gap and 3mm gap, respectively.

Table 3 RMS voltage and current, average power and electron density of the discharge corresponding to the wave forms using 1mm glass shown in Fig.5(a-f).

S.N.	Voltage V_{rms} (kV)		Discharge Current I_{rms} (mA)	Power $V_{rms} \times I_{rms}$ (Watt)	Electron density n_e ($\times 10^{17} m^{-3}$)
1	2mm gap	1.84	9.42	17.33	2.98
2		1.89	11.90	22.49	3.87
3		1.92	13.89	26.67	4.59
4	3mm gap	1.81	6.94	12.56	2.16
5		1.89	11.88	22.45	3.86
6		1.98	14.97	29.64	5.10

Table 4 RMS voltage and current, average power and electron density of the discharge corresponding to the waveforms using 3mm glass shown in Fig. 6(a-f).

S.N.	Voltage V_{rms} (kV)		Discharge Current I_{rms} (mA)	Power $V_{rms} \times I_{rms}$ (Watt)	Electron density n_e ($\times 10^{17} m^{-3}$)
1	2mm gap	2.26	4.86	10.98	1.89
2		2.38	9.52	22.66	3.90
3		2.54	11.90	30.22	5.20
4	3mm gap	2.49	4.46	11.10	1.91
5		3.00	6.84	20.52	3.53
6		3.28	9.68	31.75	5.46

5. Conclusion

In this study, electrical characteristics of DBD in air environment at atmospheric pressure were studied by measuring different parameters using circular copper electrode system. The major results obtained in this study are summarized as follows:

a) The filamentary plasma discharge in air at atmospheric pressure could be produced using high voltage power supply in a circular parallel plate electrode configuration with different electrode gap.
b) The number of filaments and their peak values depends on applied voltage. They also vary with electrode gap.
c) Electron density of discharge could be estimated using power balance method.
d) Theoretical calculation and experimental measurement of power consumed could be done using Lissajous figures.

References

[1] Balcon N, Aanesland A and Boswell R (2002). Pulsed RF Discharges, Glow and Filamentary Mode at Atmospheric Pressure in Argon. *Plasma Sources Science and Technology*. Vol. 16, No. 2, 217-225

[2] Brandenburg R, Navratil Z, Jansky J,St'ahel P and Wagner H-E (2009). The Transition Between Different Modes of Barrier Discharges at Atmospheric Pressure. *Journal of Physics D: Applied Physics*, 42: 1-10

[3] Dong-Ling B, Yun W and Min J (2018). Characterisation of Surface Dielectric Barrier Discharge Based on Pl/Al_2O_3 *Nanocomposite. Plasma Process polym: 1-12*

[4] Dramane B, Zouzou N, Moreau E, Mizuno A and Touchard G (2008). Characteristics of a DBD in Axisymmetric and Plannar Configurations: Electrical properties. *International Journal of Plasma Invironmental Science and Technology*, Vol. 2, No. 2, 89-94

[5] Gyawali H P, Shrestha S, Nakarmi N and Tyata R B (2018). Effects of Coaxial Dielectric Barrier Discharge on Water Treatment at Different Sites of Kathmandu Valley, Nepal. *Journal of Science and Engineering*, Vol. 5, No. 1, 1-6

[6] Kennedy L and Fridman A (2004). Plasma Physics and Engineering. *Tailor and Francis, New York.*

[7] Konelschatz U, Eliasson B and Egli W (1997). Dielectric-Barrier Discharges. Principle and Applications. *Journal De Physique* IV. Vol 7:47-66

[8] Kudu K, Lagstad H L and Sigmond R S (1998). Positive Point to Plane Corona Discharge forms in O_2-N_2 Mixture. *Czechosloval Journal of Physics*, Vol. 48, No. 10, 1180-1192.

[9] Liu W, Ma C, Zhao S, Chen X, Wang T, Zhao L, Li Z, Niu J, Zhu L and Chai M (2018). Exploration to Generate Atmospheric Glow Discharge Plasma in Air. *Plasma Science and Technology 20, Chinese Academy and Sciences and IOP publishing*: 1-14

[10] Lopez-Fernandez J A, Pena-Eguiluz R, Lopez-Callejas R, Marcado-Cabrera A, Valencia-Alvarado R, Munoz-Castro A and Rodriguez-Mendez B G (2017). Electrical Model of Dielectric Barrier Discharge Homogenous and Filamentary Modes. *Journal of Physics: Conference Series* 792: 1-8

[11] Pavon S (2008). Interaction Between a Surface Dielectric Barrier Discharge and Transonic Airflows. Ph.D.Thesis, *Applied Thermodynamics and Turbo-machinary Laboratory, Swiss Federal Institute of Technology, Switzerland.*

[12] Pekarek S (2012). Experimental Study of Surface DBD in Air and Its Ozone Production. *Journal of Physics D: Applied Physics*, 45: 1-9[13] Raider Y P (1991). Gas Discharge Physics. *Springer Verlag Berlin.*

[14] Rajasekaran P, Mertamann P, Bibinov N, Wandke D, Viol W and Awakowicz P (2010). Filamentary and Homogenous Modes of DBD in air: Investigation Through Plasma Characterization and Simulation of Surface Irradiation. *Plasma Processes and polymers* 7: 665-675

[15] Sun Y, Zeng M and Cui Z (2012). Research on Electrical Discharge. *Japanese Journal of Applied Physics* 51 09MF15: 1-4

[16] Tay W H, Yap S L and Wong C S (2014).Electrical Characteristics and Modeling of a Filamentary DBD in Atmospheric Air. *Sains Malaysiana*, 43(2): 583-594

[17] Tyata R B, Subedi D P and Wong C S (2016). Electrical Characterization of Dielectric Barrier Discharge. *International Journal of Pure and Applied Researches*, Vol.1(1), 1-8

[18] Tyata R B (2013). Generation, Characterization and Application of Atmospheric Pressure Glow Discharge. Ph.D. Thesis, *Department of Natural Science, School of science, Kathmandu University, Nepal*

[19] Wang C S and Zhang G X (2012). Effect of measurement Elements on Discharge Characteristics of Dielectric Barrier Discharge. *Physics Procedia*, 32: 664-668

[20] Xiaoping T, Ronde X, and Hui L (2012). Electrical Characteristics of DBDs in Atmospheric Pressure Air Using a Power Frequency Voltage Source. *Plasma Science and Technology*, Vol. 14, No. 8, 723-727

[21] Yahila A(2016). The Electrical Characteristics of the dielectric Barrier Discharges .*Physics of Plasmas*: 23: 1-11.